Optical Materials 175 (2026) 117946

Contents lists available at ScienceDirect

Optical Materials

journal homepage: www.elsevier.com/locate/optmat

Research Article

Methanol-detection by acrylate-based composite polymer film actuation

Riccardo Castagna [a,b,*], Cristiano Riminesi [a,b], Daniele E. Lucchetta [c], Fabrizio Papa [d], Gautam Singh [e], Mario Da Prada [f], Andrea Di Donato [g,**]

[a] Consiglio Nazionale delle Ricerche (CNR), Dipartimento di Scienze Umane, Sociali e Patrimonio Culturale (DSU-CNR), URT-DSU@UNICAM, Laboratorio di Scienza e Tecnologie dei Materiali per la Fotonica e la Sensoristica - Laboratory of Science and Tecnologies for Advanced Materials: Photonics and Sensors (PHOSMAT), Via Sant'Agostino, 1, Camerino, MC, 62032, Italy

[b] Consiglio Nazionale delle Ricerche (CNR), Dipartimento di Scienze Umane, Sociali e Patrimonio Culturale (DSU-CNR), Istituto di Scienza del Patrimonio Culturale (ISPC-CNR), Via Madonna del Piano, 10, Firenze, FI, 50019, Italy

[c] Università Politecnica delle Marche, DIpartimento SIMAU, Laboratorio di Opto-acustica, Via Brecce Bianche Ancona, AN, 60131, Italy

[d] Università degli Studi di Camerino, UNICAM, School of Science and Technology, Chemistry Division, Via Sant'Agostino, 1, Camerino, MC, 62032, Italy

[e] Department of Applied Physics, Amity Institute of Applied Sciences, Amity University, Noida, Uttar Pradesh, 201313, India

[f] Pra.ma, Via Pisacane, 1, Sondalo, SO, 23035, Italy

[g] Università Politecnica delle Marche, Dipartimento DII, Via Brecce, Bianche, Ancona, AN, 60131, Italy

ARTICLE INFO

Keywords:
Volatile organic compounds (VOCs)
Polymer-film actuator
Sensors
Photo-mobile polymer films
PMPs
Methanol-responsive bending

ABSTRACT

We demonstrate a proof-of-concept approach for VOC detection based on the mechanical bending of acrylate-based composite polymer films. Under ambient conditions, methanol vapours induce a rapid and reversible defor-mation of the film, which is optically observable and quantitatively described through a viscoelastic three-parameter solid model coupled to pseudo-first- order adsorption kinetics. The bending response differs markedly between methanol, water, and mixed vapours, revealing a strong dependence on sur-face adsorption dynamics. The acrylate backbone is identified as the active sensing layer, capable of transducing molecular interactions into macroscopic deflection. These findings establish acrylate polymers as a simple, low-cost platform for passive VOC-responsive materials and highlight their potential for future development into calibrated sensing devices.

1. Introduction

In recent years, polymer materials have gained significant attention in, for example, sensors [1,2], robotics [3], energy harvesting [4,5] due to their ability to undergo reversible changes in shape, molecular orientation, and/or surface topography in response to external stimuli, including electromagnetic ones [6–21]. This capability has paved the way for the development of advanced functional materials with applications in many research fields including the detection of Volatile Or-ganic Compounds (VOCs). VOCs are a class of chemicals characterized by their relatively high vapour pressures at room temperature and atmospheric pressure [22,23] which significantly impact indoor and outdoor air quality [24,25]. VOCs can result from processes such as paint degradation [26], microbial activity [27–29] and various forms of pollution. The diffusion of VOCs in living environments has notable effects on human health, which makes their detection of fundamental importance. The detection of VOCs is driving the development of sophisticated monitoring technologies in different research sectors. Methanol (MeOH) is classified as VOC. It is considered as a hazardous VOC due to its high flammability and systemic toxicity [30]. We approach to VOCs detection starting from MeOH detection and involves the use of a double-layered-like thin film technology. The thin film proposed here reversibly responds to MeOH-VOC by bending, offering a novel method for detecting and studying these compounds. This peculiar feature offers possibility for new applications, such as smart actuator materials and en-ergy harvesting technologies. In detail, we explore the possibility of using a previously developed class of acrylate-based composite photo-mobile poly-mer (PMP) films [4] for VOCs detection. PMP is formed by a light-induced self-assembling polymerization process which results in a sort of asymmetric double-layered film structure. The film is mainly representable as made of two distinct parts: a multi-crosslinked acrylate which is the supporting back-bone structure

* Corresponding author. Consiglio Nazionale delle Ricerche (CNR), Dipartimento di Scienze Umane, Sociali e Patrimonio Culturale (DSU-CNR), Istituto di Scienza del Patrimonio Culturale (ISPC-CNR), Via Madonna del Piano, 10, Firenze, 50019, FI, Italy.

** Corresponding author.

E-mail addresses: riccardo.castagna@cnr.it (R. Castagna), a.didonato@staff.univpm.it (A. Di Donato).

https://doi.org/10.1016/j.optmat.2026.117946

Received 20 September 2025; Received in revised form 5 February 2026; Accepted 6 February 2026

Available online 14 February 2026

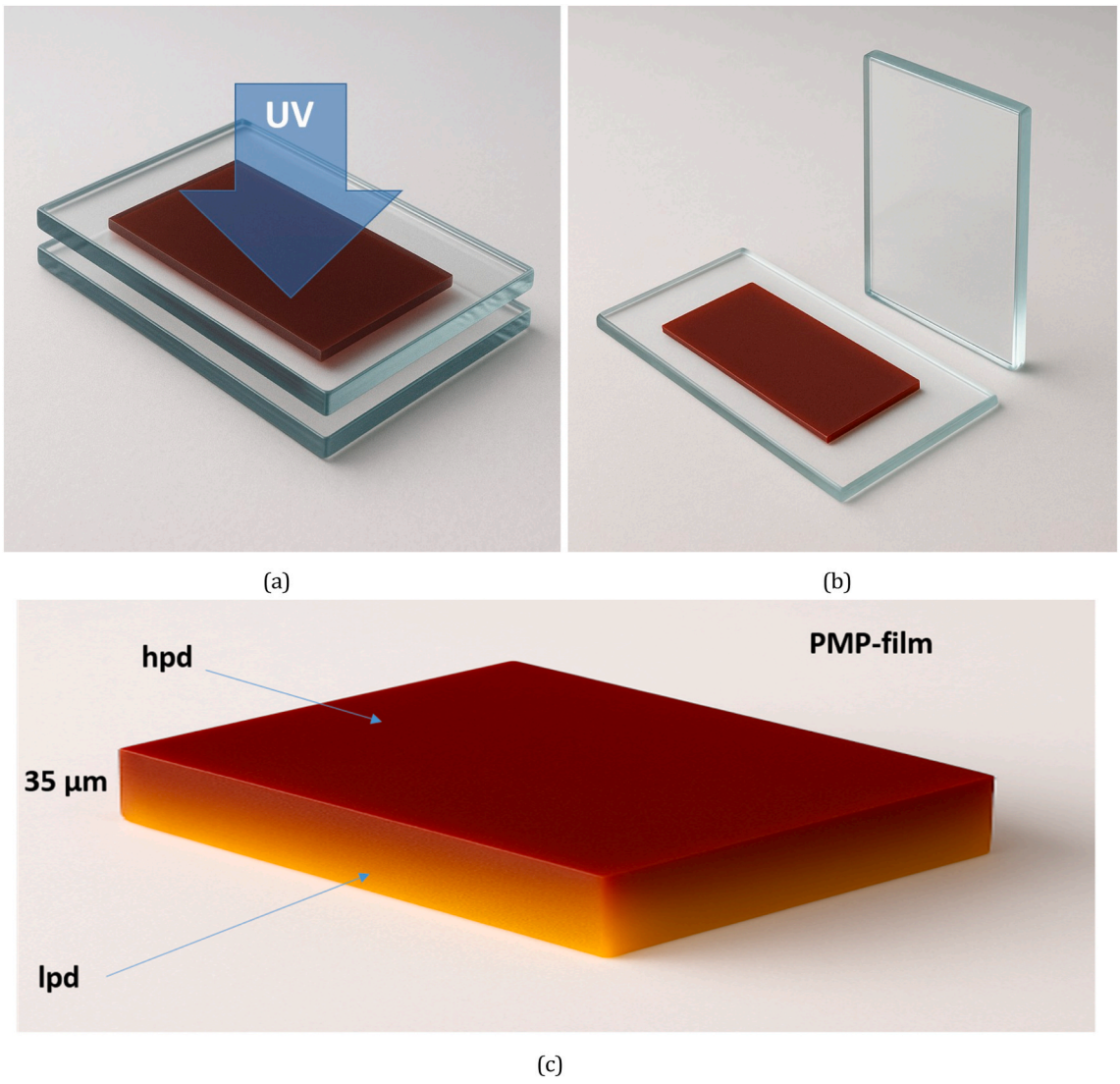

Fig. 1. 1a) UV irradiation of a PMP mixture resulting in a self assembled film con-stituted by an acrylate-rich layer and a doped 4AMP-NVP rich region, (b) After UV exposure the cover glass is remvoed and the PMP film is ready to be used. 1c) self assem-bled film constituted by an acrylate-rich layer and a doped 4AMP-NVP rich region. hpd = higher-polymerization degree; lpd = lower polymerization degree.

and a photo-thermo-mobile layer made by vinyl monomers doped with 4-amino-phenol oxidized in presence of metal oxide. This latter layer can be considered as the motor of the system. The result is a polymer film that bends under light by a photo-thermal process [6,19–21,31,32]. This allows a film deflection even under very low-intensity light. Resuming: the PMPs have the ability to convert light into heat, and heat into mechan-ical work. Surprisingly, PMPs macroscopically bend also when exposed to VOC, with a noticeable sensitivity to methanol. Macroscopic bending can be detected by using a standard camera. The present study is intended as a proof-of-concept demonstration of VOC-induced bending in acrylate-based polymer films. We focus on methanol and methanol–water mixtures to estab-lish the physical mechanism and differential response with respect to water under ambient-pressure exposure. A broader VOC panel and full metrolog-ical characterization (calibration curves versus partial pressure, LOD and dynamic range) will be addressed in future dedicated investigations using controlled VOC delivery. This work is intended as a proof-of-concept and does not attempt to determine absolute vapour concentrations or metrologi-cal calibration parameters.

2. Results and discussion

Materials and techniques used to fabricate and study acrylate-based PMP films are reported in the experimental part. Acrylate-based PMP films are multifunctional compounds. They can be patterned using holography [6,7,19] or molding [31], and are capable of bending not only when exposed to light [4] or heat [32] but also, as shown here, in response to low partial-pressure vapours of small molecules, such as VOCs or water (ddH_2O). Schematically, the PMP self-assembles during the photo-polymerization process, starting from an organic mixture, to form a sort of two-layered film (see Fig. 1; [4]) and the light coming from only one side of the sample are responsible for a fast asymmetrical photo-polymerization process [4].

When exposed to MeOH vapour, the PMP film bends with a fixed polarity set by its asymmetric structure, i.e., the bending direction is independent of whether the VOC source is placed on the left or on the right side of the sample. The bending polarity can be reversed only by physically flipping the film (i.e., exchanging the exposed face).

The PMP-film consists of a thin layer of multi-reticulated acrylate which forms its structural skeleton, while the driving force of the system is given by an acrylate layer doped with 4-AMP-NVP (see Experimental).

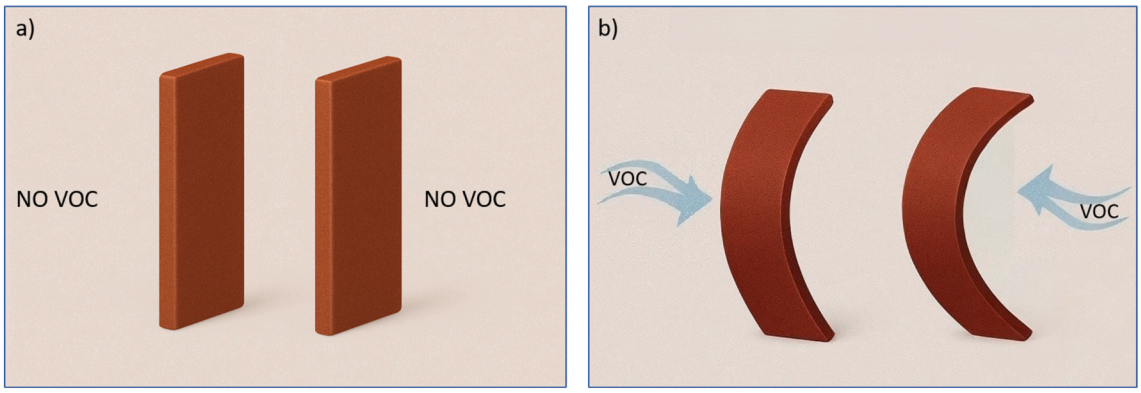

Fig. 2. Bending of the PMP film when asymmetrically exposed to two VOC sourcesv-coming from different positions. The bending direction is independent from the source position. The bending polarity is fixed by film orientation and reverses only upon flipping the film. Scale bar: film length = 1 cm. Environmental conditions: 23 ± 1 °C, RH 50 ± 5%, 1 atm.

In this study, we made the hypothesis that the effective area of the PMP in solvent detection (the surface sensitive to the solvent) is the one with the higher degree of polymerization (in other words, the one with the higher content of DPHPHA; see Supporting Information of R. Castagna et al., Adv. Mater. 2017).

We tested the sensitivity of the PMP-film obtained to detect MeOH and/or ddH_2O. In the experiment reported in Fig. 3, the vapours flowing-out from a small vessel holding solvents, such as MeOH or a MeOH-ddH_2O mixture, are used to induce bending in the acrylate-based PMP film. Fig. 3(a) shows four video frames acquired at different times by using a concen-tration of 9 : 1 MeOH:ddH_2O. All exposures were performed under ambient conditions, thus generating low partial-pressure methanol vapours without mass-flow control, consistent with the proof-of-concept scope of this work.

The mechanical response of the film is recorded on a video by using a standard camera, and each frame is analyzed with a tracking software (see Experimental Section) to determine the film's deflection as a function of time. Experimental data describing the deflection of the PMP-film when exposed to two different types of analytes in three different relative concentrations: (1) 1:9, (2) 1:1 and 9:1 mixture of MeOH and ddH_2O are reported in Fig. 3(b). The results highlight the film's distinct bending behaviors depending on the presence of MeOH-VOC. In particular, the fastest response is triggered by exposure to the highest relative concentration of methanol, while the slow-

est is dictated by water. An intermediate response speed is observed for 1:1 concentrations of MeOH and ddH_2O. Reproducibility was evaluated over 10 consecutive bending–recovery cycles, showing no measurable degradation in bending amplitude or onset time. After removal of the VOC source, the film returned to its baseline position within 3–5 min, with no permanent deformation observed. Reasonably, in the first few seconds, the response is driven by MeOH (probably the methanol molecules occupy the active sites on the surface of the polymer). The red curve takes about 60 s to reach a plateau. The experimental data fit with the theoretical model de-tailed in Ref. [33] during the deformation and relaxation phases, in order to understand the molecular adsorption kinetics. In principle, different VOCs may lead to different time-dependent responses; however, in the present work we restrict the analysis to methanol and methanol–water mixtures, without making claims of general VOC selectivity. This approach also allowed-us to separate the mechanical viscoelastic parameters from those describing the molecular-surface interaction. In particular, when modeling the kinetic pro-cess, we employed a "pseudo first-order" (PFO) model, which includes two basic assumptions [34]: first, the number of adsorbed molecules at equilib-rium is proportional to the ambient concentration of the analyte; second, the rate of adsorption is proportional to the difference between the amount of molecules adsorbed at equilibrium and the current amount adsorbed on the surface. The kinetics of adsorption are studied by observing the mechanical.

Response of the film during its deformation under VOC exposure. In this case, the viscoelastic properties of the film introduce an additional degree of complexity. This aspect is generally not considered in the well-known Stoney's equation [35,36], which is typically applied to study the mechanical response of thin films in the presence of adsorption-induced surface stress. To describe the bending of the viscoelastic film loaded with surface stress, we used an accurate and general model in which the polymer is described as a three-parameter solid [37]. In this model the time response of the biaxial stress $\sigma(t)$ is related to the biaxial strain $\varepsilon(t)$ by the equation:

$$\sigma(t) + \tau_r \frac{d\sigma}{dt} = M_\infty \varepsilon(t) + \tau_r M_0 \frac{d\varepsilon}{dt} \tag{1}$$

where M_∞ and M_0 are the relaxed and the initial biaxial modulus, respectively, and τ_r is the relaxation time constant. The advantage of this model is the simplicity, while still capturing the general characteristics of any vis-coelastic material. Assuming a film thickness very small compared to other geometrical film dimensions, the deflection of the film along the direction z (see Fig. 2) under uniform surface stress is described by the analytical equation [33]:

$$w = -\frac{L^2}{2}\frac{6\sigma_{ss}}{M_\infty h^2}\left(1 + \frac{(\bar{\tau}-1)\bar{M}}{1-\bar{M}\bar{\tau}}e^{-\frac{t}{\tau_s}} - \frac{1-\bar{M}}{1-\bar{M}\bar{\tau}}e^{-\bar{M}\frac{t}{\tau_r}}\right)u_s(t) \tag{2}$$

where L is the film length, h is the thickness and σ_{ss} is the steady-state surface stress, proportional to the ambient concentration of the analyte. In addition, the dimensionless parameters are used: $\bar{M} = \frac{M_0}{M_\infty}$ and $\bar{\tau} = \frac{\tau_r}{\tau_s}$. Equation (2) is derived analytically for the case of a step-function ambient concentration $C_{amb}(t) = C_{amb}\, u_s(t)$ with $u_s(t)$ being a unit step function [33]. We optimize the experimental operating conditions to best represent the ideal exposure condition. In the three-parameter solid model, the key param-eters describing the film's viscoelastic properties are the asymptotic biaxial modulus M_∞, the initial biaxial modulus M_0, and the relaxation time con-stant τ_r. Conversely, in the PFO model, the current ambient concentration and the adsorption time constant τ_s are the main parameters describing the adsorption kinetics. The close fit between the experimental data reported in Fig. 3(b) and the empirical PFO model provides insights into the molec-ular adsorption kinetics. Based on this, the physical adsorption mechanism effectively describes the weak interaction of molecules sticking onto the sur-face of the polymer film, especially at low VOC concentrations [38]. The time-dependent response is related to the adsorption kinetics. Specifically, the deflection of the film is caused by changes in surface stress, which occur due to the adsorption of VOCs onto the exposed side of the polymer film [39–41]. The approach can be extended to other VOCs;

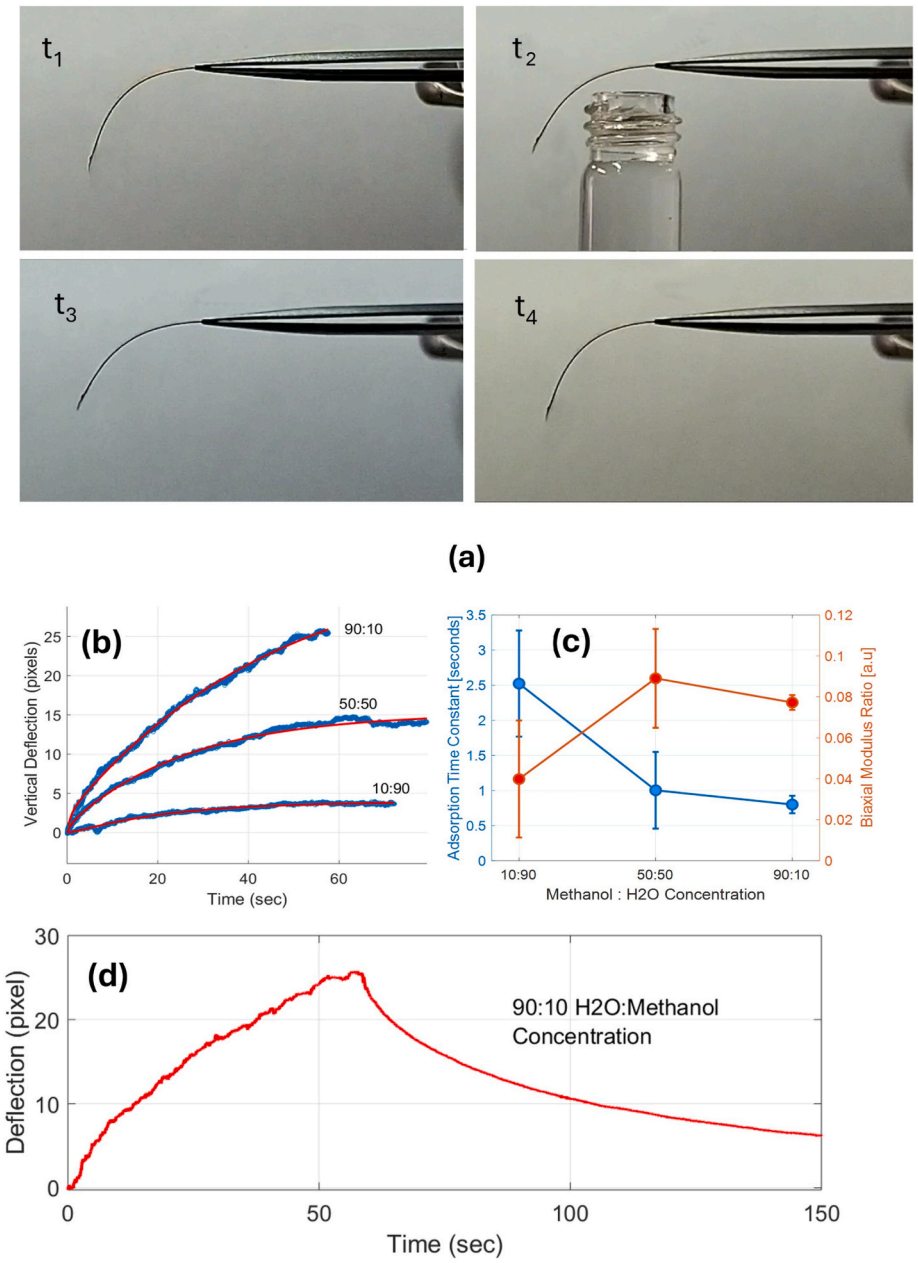

Fig. 3. (a) Sequence of frames acquired from recorded video at times $t_1 = 0$ s, $t_2 = 50$ s, $t_3 = 60$ s, $t_4 = 175$ s, highlighting the dynamic response of the polymer film under methanol exposure. Arrows indicate the bending direction. Scale bar: film length = 1 cm. Environmental conditions: 23 ± 1 °C, RH 50 ± 5%, 1 atm. (b) Experimental data describing the deflection of the PMP film when exposed to three different types of analytes: (1) 1:9, (2) 1:1 and (3) 9:1 mixture of MeOH and ddH_2O. In the inset, the adsorption time constant and the biaxial modulus ratio are reported, describing the kinetics of adsorption and the viscoelastic properties of the polymer film. The continuous lines represent the theoretical data fit given by Eq. (2).

here we quantify MeOH/H2O mixtures. The rate at which molecules are adsorbed onto the surface is quantified by the adsorption time constant, a critical parameter in the adsorption kinetics. The adsorption time constant is also correlated with the sensitivity of the polymer film and the magnitude of the deflection. As shown in Fig. 3(b), the film exhibits different deflection rates and am-plitudes depending on the solvent used. The faster the VOC molecules are adsorbed onto the surface, the quicker the temporal response and the greater the deflection amplitude of the film (see inset Fig. 3(b)). The physical ad-sorption of VOC molecules also affects the viscoelastic properties of the film, as indicated by the ratio of the biaxial modulus at different concentrations (see inset of Fig. 3(b)). This behavior suggests a possible surface contami-nation of the film under VOC exposure, which becomes more pronounced at higher adsorption rates.

According to the data shown in the inset of Fig. 3(b), the adsorption time constants for the 1:1 and 9:1 of methanol:ddH_2O relative concentrations are found to be similar, approximately 1 s and 0.8 s, respectively. However, the biaxial modulus ratio for these concentrations is nearly twice that of the 1:9 methanol:water concentration. Additionally, the curve ob-tained from the 1:1 MeOH-water mixture appears to reach the steady-state surface stress at values that are intermediate between those obtained from 1:9 and 9:1 MeOH:water concentrations. This suggests the presence of active sites on the surface of the acrylate. Such a configuration should be sensitive to small molecules, such as water and/or methanol. A competition between water and methanol in filling these active sites is evident from the analy-sis of the initial portion of the bending curves. MeOH and the MOH-water mixture produce similar responses, while higher bending values are obtained when exposed to

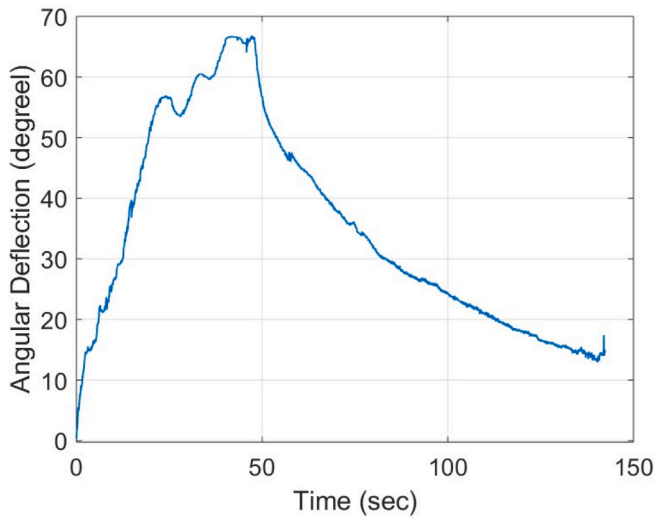

Fig. 4. Deflection response of a symmetric GPTA-acrylate film exposed to methanol vapours. The film always bends away from the VOC source. Scale bar: film length = 0.8 cm. Environmental conditions: 23 ± 1 °C, RH 50 ± 5%, 1 atm.

pure methanol. This leads to the hypothesis that even smaller quantities of methanol might be sufficient to induce a similar initial bending.

As stated above, in Fig. 3(a) is reported a sequence of video frames acquired during exposure to 1:9 MeOH:water.

We tested the hypothesis that acrylate in the PMP film is responsible for the bending triggered by VOC or water. To investigate this, we recorded the movement of a thin symmetric GPTA-acrylate film (35 μm thickness; 0.5 × 0.8 cm2) on a macroscopic scale. A typical result is shown in Fig. 4. The behavior clearly shows that the bending is caused by the acrylate film, which can reasonably be considered to be the underlying cause of the bending observed in the PMPs. The GPTA-acrylate film bends away from the VOC source (see the scheme in Fig. 5), independently of the position of the VOC with respect to the film. Finally, to show that the GPTA-based film is extremely sensitive to traces of water, we qualitatively show that the film bends in the proximity of a finger, detecting its perspiration (see video V1).

2.1. *Bending polarity: intrinsic (PMP) vs gradient-driven (GPTA)*

A key distinction emerges when comparing PMP films with symmetric GPTA-acrylate controls. PMP films exhibit an *intrinsic* bending polarity imposed by the asymmetric double-layer structure formed during photo-polymerization. Therefore, the bending direction does not depend on the.

Lateral position of the VOC source (left/right), but only on the film orienta-tion; flipping the film reverses the observed polarity.

In contrast, symmetric GPTA-acrylate films do not possess an intrinsic polarity. Their deflection is governed by adsorption-induced surface-stress gradients and is always directed away from the VOC source, independently of the lateral position of the source.

3. Conclusion

In summary, we have shown that acrylate-based PMP films exhibit a clear and reproducible bending response upon exposure to methanol vapours under ambient conditions. The bending kinetics are well captured by a viscoelas-tic three-parameter solid model coupled to pseudo-first-order adsorption dy-namics. The response differs markedly between methanol, water and mixed vapours, demonstrating a differential bending behaviour between MeOH and ddH_2O. Control experiments on symmetric GPTA-acrylate films confirm that the acrylate layer acts as the active VOC-responsive backbone of the system.

This work represents a proof-of-concept demonstration and does not at-tempt to determine absolute vapour concentrations, detection limits, or sen-sitivity curves under controlled partial pressures. Full metrological char-acterization (calibration versus partial pressure, LOD and dynamic range) and extension to a wider VOC library will be addressed in future dedicated studies using mass-flow-controlled VOC delivery. The combination of fast onset, full reversibility, and simple optical readout highlights acrylate films as promising candidates for low-cost, passive VOC-responsive materials and smart actuator platforms.

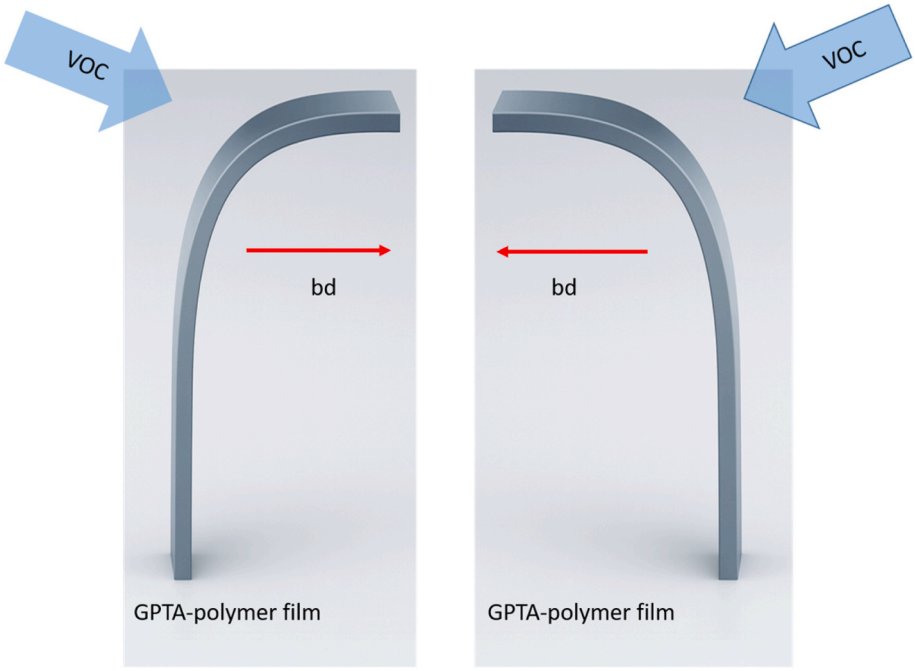

Fig. 5. Deflection responses of a GPTA-acrylate film exposed to methanol vapours are independent from the VOC source position. bd = bending direction. The arrow indicates the direction of the VOC flux. Scale bar: film length = 0.8 cm. Environmental conditions: 23 ± 1 °C, RH 50 ± 5%, 1 atm.

4. Experimental Section

4.1. Materials

- GPTA (Glycerine (PO)3 Triacrylate) from Miramer. - The follow-ing reagents are obtained from Merck: Phenylbis-(2,4,6-trimethylbenzoyl)-phosphine oxide (Irgacure 819),2,6-Bornanedione (Camphorequinone, CQ), lead(IV) oxide (PbO_2), dipentaerythritol-hydroxy-penta/hexa-acrylate (DPH- PHA), N-Vinyl-pyrrolidone (NVP), and 4-aminophenol (4AMP).

4.2. Preparation of GPTA-acrylate mixtures

To prepare the acrylate mixtures, 3 percent (w/w) of Irgacure 819 is added to 5 mL of GPTA in a small bottle. The mixture is stirred magnetically at room temperature in the dark for 24 h. After this period, the bottle is stored in darkness at room temperature until use.

4.3. Film preparation

The pre-mixed acrylate solution is sandwiched between two glass slides, forming a film approximately 35 μm thick. The assembly is then exposed to UV irradiation for 60 s, yielding a polymer film actuator ready for use.

4.4. Preparation of PMP mixture

The PMP mixture is prepared in two steps. First, 4-AMP is dissolved in NVP, with PbO_2 added to initiate a color change from transparent to dark red. This solution is stirred in the dark for 7 days. Separately, the photoinitiators (Coumarin and Irgacure 819) are mixed with DPHPHA and stirred in the dark for 24 h. The two solutions are then combined and stirred for another 24 h at room temperature (25°C) in the dark.

4.5. Preparation of PMP film

The prepared PMP mixture is introduced into a sandwich structure formed by two glass slides, separated by 35 μm spacers. Polymerization is induced using a Wisdom model XC-9262 100W UV-A-Vis lamp emitting 82,000 lu-mens for 30 min.

4.6. Preparation of GPTA-polymer film

The liquid pre-polymerized mixture is introduced into a sandwich struc-ture formed by two glass slides, separated by 35 μm spacers. Polymerization is induced using a Wisdom model XC-9262 100W UV-A-Vis lamp emitting 82,000 lumens for 30 min.

4.7. Analytical setup

The motion of the polymer actuator is recorded using a Realme 9i camera at 30 frames per second, with a video resolution of 1920x1080 pixels (full HD). All measurements were carried out at room temperature (23 ± 1 °C), ambient pressure (1 atm), and relative humidity RH 50 ± 5%. No significant fluctuations of these parameters were observed during experiments.

The PMP film, measuring 1 cm in length, 0.5 cm in width, and approxi-mately 35 μm in thickness, is placed above a small 4 ml bottle at a distance of approximately 0.5 cm. This bottle contained different mixtures of water and methanol, with methanol-to-water ratios of 9:1, 1:1, and 1:9, respectively. In the present setup, vapour exposure is generated by passive evaporation from liquid MeOH–H_2O mixtures under ambient conditions. Absolute gas-phase concentrations at the film are not measured. The reported ratios are used as relative proxies for vapour activity, suitable for proof-of-principle demon-stration but not for metrological calibration. The object tracking software is based on Labview Imaq Motion Estimation Libraries.

CRediT authorship contribution statement

Riccardo Castagna: Conceptualization, Data curation, Funding acquisition, Investigation, Methodology, Project administration, Resources, Supervision, Validation, Visualization, Writing – original draft, Writing – review & editing. **Cristiano Riminesi:** Supervision, Writing – review & editing. **Daniele E. Lucchetta:** Supervision, Writing – original draft. **Fabrizio Papa:** Supervision. **Gautam Singh:** Supervision. **Mario Da Prada:** Supervision. **Andrea Di Donato:** Formal analysis, Methodology, Software, Supervision, Writing – original draft, Writing – review & editing.

Declaration of competing interest

The authors declare that they have no known competing financial interests or personal relationships that could have appeared to influence the work reported in this paper.

Acknowledgements

This research has been supported by URT-DSU@UNICAM, Dipartimento di Scienze Umane, Sociali e del Patrimonio culturale, DSU-CNR, Consiglio Nazionale delle Ricerche, Via Sant'Agostino, 1, 62032 Camerino (MC).

Appendix A. Supplementary data

Supplementary data to this article can be found online at https://doi.org/10.1016/j.optmat.2026.117946.

Data availability

Data will be made available on request.

References

[1] S. Cichosz, A. Masek, M. Zaborski, Polymer-based sensors: a review, Polym. Test. 67 (2018) 342–348.
[2] G. Alberti, C. Zanoni, V. Losi, L.R. Magnaghi, R. Biesuz, Current trends in polymer based sensors, Chemosensors 9 (5) (2021).
[3] T. Kim, P. Kaarthik, R.L. Truby, A flexible, architected soft robotic ac- tuator for motorized extensional motion, Adv. Intelligent Systems n/a (n/a) (2024) 2300866.
[4] R. Castagna, L. Nucara, F. Simoni, L. Greci, M. Rippa, L. Petti, D.E. Lucchetta, An unconventional approach to photomobile composite poly- mer films, Adv. Mater. 29 (13) (2017) 1604800.
[5] H. Koerner, T.J. White, N.V. Tabiryan, T.J. Bunning, R.A. Vaia, Photogenerating work from polymers, Mater. Today 11 (7) (2008) 34–42, https://doi.org/10.1016/S1369-7021(08)70147-0.
[6] D.E. Lucchetta, A. Di Donato, M. Paturzo, G. Singh, R. Castagna, Light-induced dynamic holography, Micromachines 13 (2) (2022), https://doi.org/10.3390/mi13020297 cited by: 6; All Open Access, Gold Open Access, Green Open Access.
[7] D.E. Lucchetta, A. Di Donato, G. Singh, A. Tombesi, R. Castagna, Optically tunable diffraction efficiency by photo-mobile holographic composite polymer material, Opt. Mater. 121 (2021) 111612, https://doi.org/10.1016/j.optmat.2021.111612.
[8] M. Yamada, M. Kondo, J.-i. Mamiya, Y. Yu, M. Kinoshita, C.J. Barrett, T. Ikeda, Photomobile polymer materials: towards light-driven plastic motors, Angew. Chem. 120 (27) (2008) 5064–5066.
[9] J. He, Y. Zhao, Y. Zhao, Photoinduced bending of a coumarin- containing supramolecular polymer, Soft Matter 5 (2) (2009) 308–310.
[10] M. Kondo, T. Matsuda, R. Fukae, N. Kawatsuki, Photoinduced defor- mation of polymer fibers with anthracene side groups, Chem. Lett. 39 (3) (2010) 234–235.
[11] M. Kondo, M. Takemoto, T. Matsuda, R. Fukae, N. Kawatsuki, Prepa- ration and macroscopic deformation of liquid-crystalline polymer fibers crosslinked with anthracene side chains, Mol. Cryst. Liq. Cryst. 550 (1) (2011) 98–104.
[12] J. Gao, Y. He, F. Liu, X. Zhang, Z. Wang, X. Wang, Azobenzene- containing supramolecular side-chain polymer films for laser-induced surface relief gratings, Chem. Mater. 19 (16) (2007) 3877–3881.
[13] M. Kondo, M. Takemoto, R. Fukae, N. Kawatsuki, Photomobile poly- mers from commercially available compounds: photoinduced deforma- tion of side-chain polymers containing hydrogen-bonded photoreactive compounds, Polym. J. 44 (5) (2012) 410–414.

[14] T. Ube, T. Ikeda, Photomobile polymer materials with complex 3d de- formation, continuous motions, self-regulation, and enhanced process- ability, Adv. Opt. Mater. 7 (16) (2019) 1900380.
[15] T. Ikeda, T. Ube, Photomobile polymer materials: from nano to macro, Mater. Today 14 (10) (2011) 480–487, https://doi.org/10.1016/S1369-7021(11)70212-7.
[16] T.J. White, N.V. Tabiryan, S.V. Serak, U.A. Hrozhyk, V.P. Tondiglia, H. Koerner, R. A. Vaia, T.J. Bunning, A high fre- quency photodriven polymer oscillator, Soft Matter 4 (2008) 1796–1798, https://doi.org/10.1039/B805434G, 10.1039/B805434G.
[17] P. De Gennes, Possibilites offertes par la reticulation de polymeres en presence d'un cristal liquide, Phys. Lett. 28 (11) (1969) 725–726.
[18] A.S. Kuenstler, R.C. Hayward, Light-induced shape morphing of thin films, Curr. Opin. Colloid Interface Sci. 40 (2019) 70–86, https://doi.org/10.1016/j.cocis.2019.01.009, particle Systems.
[19] D.E. Lucchetta, R. Castagna, G. Singh, C. Riminesi, A. Di Donato, Spectral, morphological and dynamical analysis of a holographic grating recorded in a photo-mobile composite polymer mixture, Nanomaterials 11 (11) (2021), https://doi.org/10.3390/nano11112925.
[20] R. Castagna, A.D. Donato, G. Strangi, D.E. Lucchetta, Light con- trolled bending of a holographic transmission phase grating, Smart Mater. Struct. 31 (3) (2022), https://doi.org/10.1088/1361-665X/ac4a47, 03LT02.
[21] D.E. Lucchetta, P. Castellini, M. Martarelli, L. Scalise, G. Pandarese, C. Riminesi, G. Singh, A. Di Donato, O. Francescangeli, R. Castagna, Light-controlled rotational speed of an acoustically levitating photomo- bile polymer film, Materials 16 (2) (2023), https://doi.org/10.3390/ma16020553.
[22] M. Khatib, H. Haick, Sensors for volatile organic com- pounds, ACS Nano 16 (5) (2022) 7080–7115, https://doi.org/10.1021/acsnano.1c10827, pMID: 35511046.
[23] EPA, What are volatile organic compounds (vocs)? Tech. rep. (2024). EPA, Envirnmental Protection Agency.
[24] F. Brilli, F. Loreto, I. Baccelli, Exploiting plant volatile organic com- pounds (vocs) in agriculture to improve sustainable defense strategies and productivity of crops, Front. Plant Sci. 10 (2019) 1–8, https://doi.org/10.3389/fpls.2019.00264, cited by: 195; All Open Access, Gold Open Access, Green Open Access.
[25] X. Zhou, X. Zhou, C. Wang, H. Zhou, Environmental and human health impacts of volatile organic compounds: a perspective review, Chemosphere 313 (2023) 137489, https://doi.org/10.1016/j.chemosphere.2022.137489.
[26] M. Song, H. Chun, Species and characteristics of volatile organic com- pounds emitted from an auto-repair painting workshop, Sci. Rep. 11 (1) (2021), https://doi.org/10.1038/s41598-021-96163-4 cited by: 21; All Open Access, Gold Open Access, Green Open Access.
[27] S.U. Morath, R. Hung, J.W. Bennett, Fungal volatile organic com- pounds: a review with emphasis on their biotechnological potential, Fungal Biol. Rev. 26 (2) (2012) 73–83.
[28] L. Ling, Y. Li, K. Jiang, Y. Wang, H. Luo, W. Cheng, M. Pang, L. Feng, R. Yue, Y. Zhou, Volatile organic compounds of bacillus spp. as an emerging antifungal resource play a significant role in fruit postharvest disease control, Food Biosci. 56 (2023) 103201.
[29] Y. Guo, W. Jud, F. Weikl, A. Ghirardo, R.R. Junker, A. Polle, J.P. Benz, K. Pritsch, J.-P. Schnitzler, M. Rosenkranz, Volatile organic com- pound patterns predict fungal trophic mode and lifestyle, Commun. Biol. 4 (1) (2021) 673, https://doi.org/10.1038/s42003-021-02198-8.
[30] European Parliament and Council of the European Union, Regulation (ec) no 1272/2008 of the european parliament and of the council of 16 December 2008 on classification, labelling and packaging of substances and mixtures (clp), Off. J. Eur. Union (2008) 1–1355. Annex VI, Part 3: Methanol (CAS 67-56-1), https://eur-lex.europa.eu/legal-content/EN/TXT/?uri=CELEX:02008R1272.
[31] R. Castagna, M. Rippa, F. Simoni, F. Villani, G. Nenna, L. Petti, Plasmonic photomobile polymer films, Crystals. 10 (8) (2020), https://doi.org/10.3390/cryst10080660.
[32] R. Castagna, C. Riminesi, M.S. Pianesi, S. Sabbatini, A. Di Donato, G. Singh, O. Francescangeli, E. Cantisani, P. Castellini, D.E. Luc- chetta, Development of a quartz-based photo-mobile polymer film for controlled motion triggered by light or heat, Materials. 16 (8) (2023), https://doi.org/10.3390/ma16083046.
[33] M.J. Wenzel, F. Josse, S.M. Heinrich, Deflection of a viscoelastic can- tilever under a uniform surface stress: applications to static-mode mi- crocantilever sensors undergoing adsorption, J. Appl. Phys. 105 (6) (2009).
[34] T.A. Saleh, Chapter 3 - kinetic models and thermodynamics of adsorp- tion processes: classification, in: T.A. Saleh (Ed.), Surface Science of Adsorbents and Nanoadsorbents, vol. 34, Elsevier, 2022, pp. 65–97, https://doi.org/10.1016/B978-0-12-849876-7.00003-8, of Interface Science and Tech- nology.
[35] G.G. Stoney, The tension of metallic films deposited by electrolysis, Proc. R. Soc. Lond. - Ser. A Contain. Pap. a Math. Phys. Character 82 (553) (1909) 172–175.
[36] R.W. Hoffman, Mechanical Properties of Non-metallic Thin Films, Springer US, Boston, MA, 1976, pp. 273–353.
[37] W. Flügge, W. Flügge, Viscoelastic Models, Viscoelasticity, 1975, pp. 4–33.
[38] E. McCash, Adsorption and desorption, Surface Chemistry (2001) 81–84.
[39] N.V. Lavrik, M.J. Sepaniak, P.G. Datskos, Cantilever transducers as a platform for chemical and biological sensors, Rev. Sci. Instrum. 75 (7) (2004) 2229–2253.
[40] Z. Hu, T. Thundat, R.J. Warmack, Investigation of adsorption and absorption-induced stresses using microcantilever sensors, J. Appl. Phys. 90 (1) (2001) 427–431.
[41] D.W. Dareing, T. Thundat, Simulation of adsorption-induced stress of a microcantilever sensor, J. Appl. Phys. 97 (4) (2005) 043526, https://doi.org/10.1063/1.1853496.